



Intratracheal instillation of single-wall carbon nanotubes in the rat lung induces time-dependent changes in gene expression

Katsuhide Fujita, Makiko Fukuda, Hiroko Fukui, Masanori Horie, Shigehisa Endoh, Kunio Uchida, Mototada Shichiri, Yasuo Morimoto, Akira Ogami & Hitoshi Iwahashi

To cite this article: Katsuhide Fujita, Makiko Fukuda, Hiroko Fukui, Masanori Horie, Shigehisa Endoh, Kunio Uchida, Mototada Shichiri, Yasuo Morimoto, Akira Ogami & Hitoshi Iwahashi (2015) Intratracheal instillation of single-wall carbon nanotubes in the rat lung induces time-dependent changes in gene expression, *Nanotoxicology*, 9:3, 290-301, DOI: [10.3109/17435390.2014.921737](https://doi.org/10.3109/17435390.2014.921737)

To link to this article: <https://doi.org/10.3109/17435390.2014.921737>



© 2015 The Author(s). Published by Taylor & Francis.



[View supplementary material](#)



Published online: 09 Jun 2014.



[Submit your article to this journal](#)



Article views: 1888



[View related articles](#)



[View Crossmark data](#)



Citing articles: 10 [View citing articles](#)

ORIGINAL ARTICLE

Intratracheal instillation of single-wall carbon nanotubes in the rat lung induces time-dependent changes in gene expression

Katsuhide Fujita^{1,2}, Makiko Fukuda², Hiroko Fukui¹, Masanori Horie³, Shigehisa Endoh², Kunio Uchida⁴, Mototada Shichiri⁵, Yasuo Morimoto³, Akira Ogami³, and Hitoshi Iwahashi⁶

¹Research Institute of Science for Safety and Sustainability, National Institute of Advanced Industrial Science and Technology (AIST), Tsukuba, Japan, ²Technology Research Association for Single Wall Carbon Nanotubes (TASC), Higashi, Tsukuba, Japan, ³Institute of Industrial Ecological Sciences, University of Occupational and Environmental Health, Kitakyushu, Japan, ⁴Nanosystem Research Institute, AIST, Tsukuba, Japan, ⁵Health Research Institute, AIST, Ikeda, Japan, and ⁶Faculty of Applied Biological Sciences, Gifu University, Gifu, Japan

Abstract

The use of carbon nanotubes in the industry has grown; however, little is known about their toxicological mechanism of action. Single-wall carbon nanotube (SWCNT) suspensions were administered by single intratracheal instillation in rats. Persistence of alveolar macrophage-containing granuloma was observed around the sites of SWCNT aggregation at 90 days post-instillation in 0.2-mg- or 0.4-mg-injected doses per rat. Meanwhile, gene expression profiling revealed that a large number of genes involved in the inflammatory response were markedly upregulated until 90 days or 180 days post-instillation. Subsequently, gene expression patterns were dramatically altered at 365 days post-instillation, and the number of upregulated genes involved in the inflammatory response was reduced. These results suggested that alveolar macrophage-containing granuloma reflected a characteristic of the histopathological transition period from the acute-phase to the subchronic-phase of inflammation, as well as pulmonary acute phase response persistence up to 90 or 180 days after intratracheal instillation in this experimental setting. The expression levels of the genes *Ctsk*, *Gcgr*, *Gpnmb*, *Lilrb4*, *Marco*, *Mreg*, *Mt3*, *Padi1*, *Slc26a4*, *Spp1*, *Tnfsf4* and *Trem2* were persistently upregulated in a dose-dependent manner until 365 days post-instillation. In addition, the expression levels of *Atp6v0d2*, *Lpo*, *Mmp7*, *Mmp12* and *Rnase9* were significantly upregulated until 754 days post-instillation. We propose that these persistently upregulated genes in the chronic-phase response following the acute-phase response act as potential biomarkers in lung tissue after SWCNT instillation. This study provides further insight into the time-dependent changes in genomic expression associated with the pulmonary toxicity of SWCNTs.

Keywords

Fiber toxicology, genomics, nanotoxicology, nanotubes

History

Received 11 September 2013

Revised 2 May 2014

Accepted 02 May 2014

Published online 9 June 2014

Introduction

In recent years, the use of carbon nanotubes (CNTs) as carbon-based nanomaterials has increased and is expected to expand into more diverse industrial fields (e.g. electronic or constructional materials) owing to their extraordinary thermal conductivity, as well as their mechanical and electrical properties. However, with increasing development of nanotechnology, concern about the pulmonary toxicity of CNTs has also grown (Stern & McNeil, 2008). The health impact to workers who are exposed to CNTs during manufacturing has been increasing; however, little is known about their toxicological mechanism of action. Poland et al. (2008) reported that intraperitoneal administration of long and straight multi-wall carbon nanotube (MWCNT) fibers in

rodents resulted in asbestos-like pathogenic responses. Recent *in vitro* studies have indicated the cytotoxicity of MWCNTs in human lung or bronchial epithelial cell culture systems (Cavallo et al., 2012; Haniu et al., 2013; Hirano et al., 2010). The pulmonary toxicity of MWCNTs in *in vivo* rodent models has also been reported (Ma-Hock et al., 2013; Mitchell et al., 2007; Morimoto et al., 2012a; Porter et al., 2013; Treumann et al., 2013; Urankar et al., 2012). A 90-day inhalation toxicity study with MWCNTs performed according to the Organization for Economic Co-operation and Development (OECD) test guidelines showed that increased lung weights, pronounced multifocal granulomatous inflammation, diffuse histiocytic and neutrophilic inflammation, and intra-alveolar lipoproteinosis were observed in lung and lung-associated lymph nodes at 0.5 mg/m³ and 2.5 mg/m³ (Ma-Hock et al., 2009). A 13-week nose-only inhalation study with MWCNTs demonstrated that the induced pathological changes are consistent with overload-related phenomena (Pauluhn, 2010). On the other hand, *in vitro* cytotoxicity assessment of single-wall carbon nanotubes (SWCNTs) on human lung or bronchial epithelial cell lines was demonstrated (Davoren et al., 2007; Fujita et al., 2013; Sargent et al., 2012). *In vivo* experimental studies of rat lungs after intratracheal instillation of SWCNTs have been conducted to evaluate their acute pulmonary

This is an Open Access article distributed under the terms of the Creative Commons Attribution-NonCommercial-NoDerivatives License (<http://www.ncbi.nlm.nih.gov/projects/geo/>), which permits non-commercial re-use, distribution, and reproduction in any medium, provided the original work is properly cited, and is not altered, transformed, or built upon in any way.

*Corresponding author: Katsuhide Fujita, Fax: +81-298-861-8415. E-mail: ka-fujita@aist.go.jp

toxicity in rodents. Bronchoalveolar lavage fluid (BALF) analysis revealed that exposure to SWCNTs (5 mg/kg rat) produced transient inflammatory and cell injury effects until one month after instillation (Warheit et al., 2004). In the impurity-free SWCNT-exposed group (2 mg/kg rat), acute lung inflammation and subsequent pulmonary granuloma accompanied by increased lung weights was observed, but no evidence of fibrosis, atypical lesions or tumor-related findings were observed until six months after instillation (Kobayashi et al., 2011). In our previous study, histopathological examination, BALF analysis and enzyme-linked immunosorbent assay (ELISA) demonstrated that persistent pulmonary inflammation was observed in rat lungs until six months after instillation of SWCNTs (0.2 mg or 0.4 mg per rat) (Morimoto et al., 2012b). These intratracheal instillation studies have primarily examined the acute-phase inflammatory response and recovery after instillation of SWCNTs. However, the long-term effects of SWCNTs on pulmonary toxicity after the acute-phase inflammatory response remain unexplained.

Gene expression analysis is expected to elucidate the toxicological effects of nanomaterials relevant to specific histopathological phenotypes. We have previously analyzed gene expression profiles in rat lungs after intratracheal instillation of C₆₀ fullerenes (Fujita et al., 2009a, 2010). The gene expression profiles demonstrated marked correspondence with results from other conventional methods such as immunohistochemical and BALF cell analysis. Guo et al. (2012) reported on the identification of MWCNT-induced gene expression patterns in a mouse model and determined that similar gene expression patterns in humans are associated with increased risk for lung cancer initiation and progression. These results suggest that comprehensive gene expression analysis can be useful in assessing the effect of nanomaterials on biological systems.

In this study, we performed DNA microarray-based gene expression profiling of the rat lung after intratracheal instillation with SWCNT suspensions at low- and high-injected doses (0.2 mg and 0.4 mg, respectively) in each rat. The expression levels of representative genes involved in the inflammatory response, response to oxidative stress and apoptosis after low- or high-dose intratracheal instillation of SWCNTs were determined. Gene ontology (GO) analysis was conducted to exhibit the alteration of gene expression patterns induced by SWCNTs in a time-dependent manner (from 3 to 754 days post-instillation). In addition, the expressed genes that were highly upregulated with SWCNTs until 754 days after intratracheal instillation were screened in order to identify potential biomarkers in lung tissues after SWCNT instillation. We validated the observation that gene expression was persistently upregulated by SWCNTs in the chronic-phase response by immunostaining analysis. The gene expression data presented herein are expected to provide further insight into the pulmonary toxicity of SWCNTs at the transcriptional level, together with the histopathological findings.

Materials and methods

Test materials

SWCNTs, synthesized by the catalytic chemical vapor deposition method, were obtained from Nikkiso Co., Ltd. (Tokyo, Japan). A detailed description of the characterization of bulk SWCNTs was provided in our previous report (Morimoto et al., 2012b). The geometric mean diameter of the tubes was 1.8 nm, and the specific surface area of the bulk SWCNTs was 877.7 m²/g, as measured by using the BET method (Autosorb-1-C; Quantachrome Instruments; Boynton Beach, FL). The diameter and length of the dispersed SWCNTs was 44 nm (range, 15–152 nm) and 0.69 µm (range, 0.18–3.3 µm), respectively. Bulk SWCNTs were immersed for 30 min in an ethanol-based

aqueous solution, which assisted in hydrophilizing SWCNTs using a planetary ball mill at a rotating speed of 450 rpm (P-6, FRITSCH; Idar-Oberstein, Germany). Next, fructose was added to the treated SWCNTs to assist in the milling and debundling of SWCNTs, and the mixture was ground for an additional 30–60 min using a planetary ball mill. The SWCNTs were filtered through a membrane filter (1.0-µm pore size), and the fructose on the surface was washed away with hot water. The recovered SWCNTs were dispersed into an aqueous solution of 0.5 mg/mL Triton X-100 by ultrasonication for 30 min using a homogenizer (Branson Ultrasonics, Danbury, CT). The suspension of SWCNTs was separated, and the constituents were classified by centrifugation at 3000–20 000 × g, which were used for the animal tests after the concentration of the SWCNTs in the suspension was adjusted to a maximum of 1 mg/mL. The geometric mean diameter and length of the SWCNTs in the distilled water including 0.1% Triton X-100 was 44 nm and 0.69 µm, respectively. The Fe content (13 700 ppm) in the dispersed SWCNTs was measured using inductively coupled plasma mass spectrometry (ICP-MS) (Morimoto et al., 2012b).

Animals

Nine-week-old male Wistar rats purchased from Hokudo Co., Ltd. (Sapporo, Japan) were stratified into three groups (*n* = 6 per group per time point). SWCNTs were intratracheally administered into rats in a single injection (0.2 mg or 0.4 mg SWCNT per rat). The vehicle control groups were administered 0.1% Triton X-100 per rat. After intratracheal instillation treatment, rats were housed within polycarbonate cages at a controlled temperature of 22 °C with a chow diet *ad libitum*, and were dissected at 3, 7, 30, 90, 180, 365 and 754 days post-instillation. Lungs of anesthetized rats were perfused with physiological saline, excised and subjected to morphological observation, histopathological findings and comprehensive gene expression microarray analysis. All procedures and animal handling were performed according to the guidelines described in the Japanese Guide for the Care and Use of Laboratory Animals as approved by the Animal Care and Use Committee, National Institute of Advanced Industrial Science and Technology, Tokyo, Japan.

Experimental design

SWCNTs (0.2 mg or 0.4 mg) were suspended in 0.4 mL of 0.1% Triton X-100 in distilled water. Each material suspension was intratracheally instilled one time in rats. After the instillation, the viability and general condition of the rats were observed once a day until dissection. The body weight of each rat was measured before instillation and at 3, 7, 30, 90, 180, 365 and 754 days post-exposure. The average rat body weight before the instillation treatment was approximately 270 g. Measurements of the organ weight of the lung, liver and brain in six rats per group at each time point were performed at 3, 7, 30, 90, 180, 365 and 754 days post-exposure. Three groups were analyzed: the vehicle control (0.1% Triton X-100 per rat; vehicle control) and SWCNTs in the low-dose (0.2 mg SWCNTs per rat; L-SWCNT) or high-dose (0.4 mg SWCNTs per rat; H-SWCNT) groups. The animals were dissected at 3, 7, 30, 90, 180, 365 and 754 days post-exposure.

RNA extraction and DNA microarray

The right lungs (*n* = 4 per group per time point) were homogenized using QIAzol lysis reagent with a TissueRuptor (Qiagen; Tokyo, Japan). Total RNA from the homogenates was extracted using the RNeasy Midi Kit (Qiagen) following the manufacturer's instructions. RNA was quantified using a NanoDrop 2000 spectrophotometer (Thermo Fisher Scientific

Inc.; Waltham, MA), and the quality of the samples was monitored with the Agilent 2100 Bioanalyzer (Agilent Technologies; Santa Clara, CA). Cyanine-3-labeled cRNA was prepared from RNA using the One-Color Low RNA Input Linear Amplification PLUS Kit (Agilent Technologies) according to the manufacturer's instructions, followed by RNeasy column purification (Qiagen). Each labeled cRNA probe was used separately for hybridization to a Whole Rat Genome Microarray 4 × 44 K (G4131F; Agilent Technologies), and hybridization was performed at 65 °C for 17 h. Hybridized microarray slides were washed according to the manufacturer's instructions and were scanned with an Agilent DNA Microarray Scanner (G2565BA; Agilent Technologies) at 5-micron resolution. The scanned images were analyzed numerically using the Agilent Feature Extraction Software version 10.7.3.1 (Agilent Technologies).

Microarray data analysis

Normalized data were analyzed using GeneSpring GX version 11.5.1 software (Agilent Technologies). Log fold-changes represent the ratio of the normalized intensity values of SWCNT-exposed lung samples to the normalized intensity value of vehicle control lung samples. Genes displaying log fold-change values equal to or greater than 1 were considered to be upregulated genes, whereas those displaying values equal to or less than −1 were considered to be downregulated genes. Gene expression data for each of the experimental groups were deposited in the Gene Expression Omnibus database (Accession number GSE50664; <http://www.ncbi.nlm.nih.gov/projects/geo/>). The web-based application GOstat (<http://gostat.wehi.edu.au/>) was used to identify statistically over-represented GO terms (Beissbarth & Speed, 2004) with the Rat Genome Database (RGD; <http://rgd.mcw.edu/>). Differences between the control and experimental groups were evaluated using the unequal variance Welch *t* test, which is suitable regardless of whether two groups have similar or dissimilar variance. *p* Values less than or equal to 0.05 were considered statistically significant.

Validation of gene expression data using quantitative real-time polymerase chain reaction

Total RNA was transcribed into cDNA (High-Capacity RNA-to-cDNA™ Kit; Life Technologies, Tokyo, Japan). Quantitative real-time polymerase chain reaction (qRT-PCR) assays were performed using TaqMan (Single Tube TaqMan® Gene Expression Assays; Life Technologies) according to the manufacturer's protocol. All experiments were performed in a StepOnePlus™ Real-Time PCR Systems (Life Technologies). All expression data were normalized to endogenous control *18S rRNA* expression.

Histopathology and immunohistochemistry

After the rats were sacrificed, their lungs were rapidly removed in a cold room and processed for histopathological studies or biochemical analysis. Next, lung tissues were fixed in 4% buffered paraformaldehyde, followed by embedding in paraffin, and the sections were stained with hematoxylin and eosin or Masson's trichrome staining. The digital images of each lung section focused on the alveoli, alveolar wall, bronchiole and the vessels for histopathological evaluation.

Immunohistochemical analysis was performed in paraformaldehyde-fixed paraffin sections by staining with rabbit monoclonal anti-matrix metalloproteinase 12 (MMP12) (Abcam; Cambridge, UK), rabbit monoclonal anti-MMP7 (Cell Signaling Technology, Inc.; Danvers, MA) or mouse monoclonal anti-osteopontin (SPP1) (Novus Biologicals, LLC; Littleton, CO) in Tris-buffered

saline (TBS) following deparaffinization. Antibody binding was detected by using horseradish peroxidase-conjugated with biotinylated secondary antibody and developed with 3,3'-diaminobenzidine (DAB).

Statistical analysis

All numerical values are represented as the mean ± SD. Statistically significant differences between the data for the treated samples and the untreated controls were determined by analysis of variance (ANOVA) using the Dunnett or Steel test for multiple comparisons.

Results

Body and lung weight and general condition

Statistically significant differences in the body weights of experimental animals were observed between the H-SWCNT group and the vehicle control group at 3 days ($p < 0.05$), 180 days ($p < 0.05$) and 365 days ($p < 0.01$) post-instillation (Figure 1). By contrast, statistically significant differences in lung weight were not observed between any of the experimental groups and the vehicle control group (data not shown). No clinical signs, such as abnormal behavior and irregular respiration, were observed during the observation period in any of the groups. The total number of deaths observed was the following: one in the control vehicle group, two in the L-SWCNT group and three in the H-SWCNT group. In the control vehicle group, a rat that experienced a reduction in body weight was slaughtered at 704 days post-instillation. In the L-SWCNT group, a rat that experienced a reduction in body weight and a rat with swelling in the nasal region were slaughtered at 506 days and 704 days post-instillation, respectively. In the H-SWCNT group, three rats that experienced a reduction in body weight were slaughtered at 459, 569 and 587 days post-instillation, respectively.

Anatomical observations

The SWCNT aggregates (black patches) were observed around bronchi or bronchioles in dissected lungs in both of the SWCNT

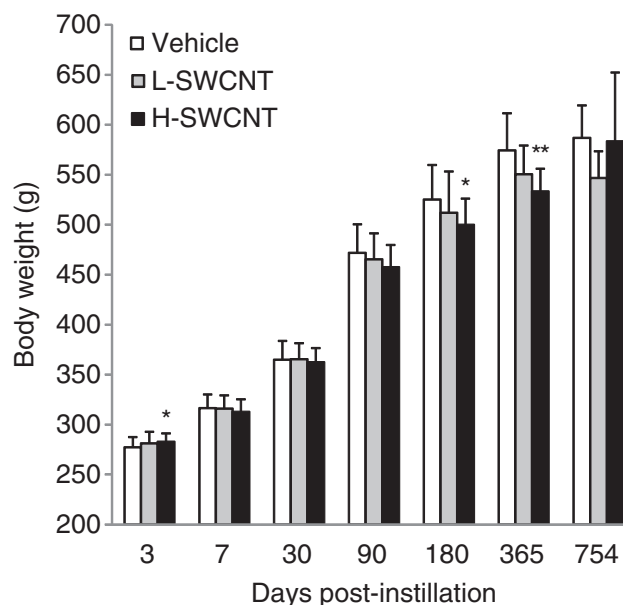


Figure 1. Body weight of rats after intratracheal instillation of SWCNTs: the vehicle control (0.1% Triton X-100 per rat; vehicle control) and the SWCNTs in the low-dose (0.2 mg SWCNTs per rat; L-SWCNT) or high-dose (0.4 mg SWCNTs per rat; H-SWCNT) groups. Values are mean ± SD. * $p < 0.05$, ** $p < 0.01$ (vs. each vehicle control group).

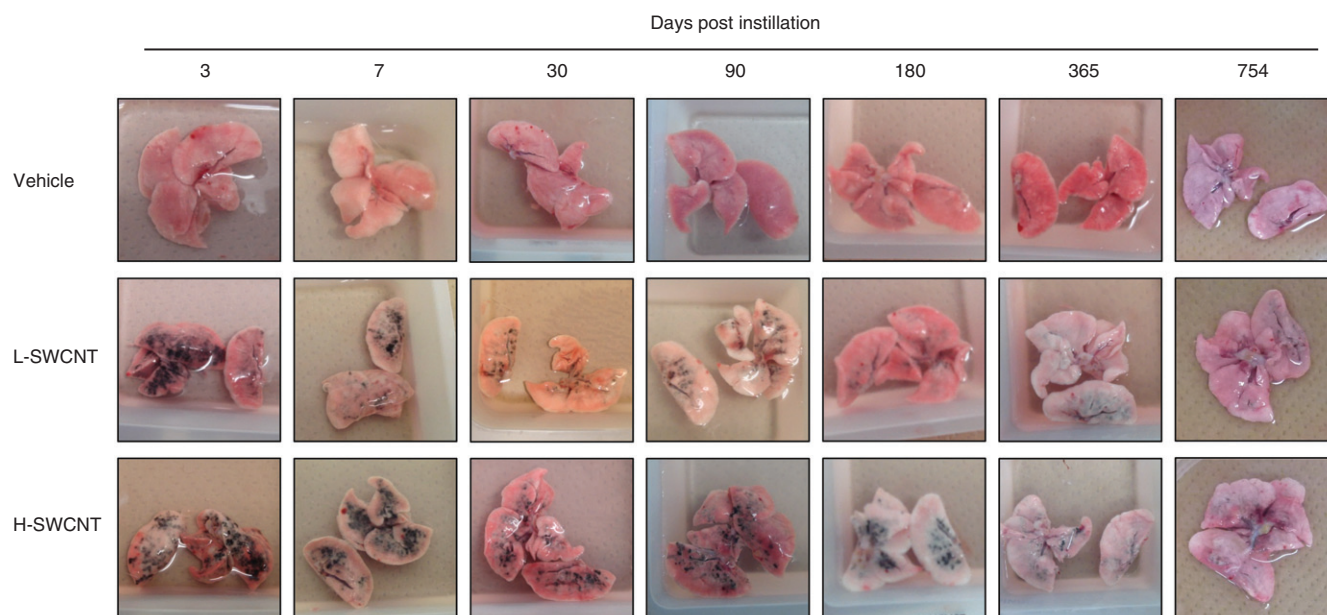


Figure 2. The dissected lungs from a rat exposed to SWCNTs at 3, 7, 30, 90, 180, 365 and 754 days post-instillation. The lungs were dissected at each post-instillation time in the three groups: the vehicle control (0.1% Triton X-100 per rat; vehicle control) and the SWCNTs in the low-dose (0.2 mg SWCNTs per rat; L-SWCNT) or high-dose (0.4 mg SWCNTs per rat; H-SWCNT) groups.

Table 1. Histopathological findings in the lung tissues intratracheally instilled with vehicle control, L-SWCNTs or H-SWCNTs.

Days post-instillation	Findings	Vehicle	L-SWCNT	H-SWCNT
3 days	SWCNTs in alveoli, alveolar wall or bronchiole	—	+	++
7 days	SWCNTs in alveoli, alveolar wall or bronchiole	—	+	++
30 days	SWCNTs in alveoli, alveolar wall or bronchiole	—	+	++
	Fibrin deposition	—	—	+
90 days	SWCNTs in alveoli, alveolar wall or bronchiole	—	+	++
	Fibrin deposition	—	—	+
	Granuloma	—	—	+
180 days	SWCNTs in alveoli, alveolar wall or bronchiole	—	+	+
	Fibrin deposition	—	—	—
	Granuloma	—	+	±
365 days	SWCNTs in alveoli, alveolar wall or bronchiole	—	+	+
	Fibrin deposition	—	—	—
	Granuloma	—	—	—
754 days	SWCNTs in alveoli, alveolar wall or bronchiole	—	+	+
	Fibrin deposition	—	—	—
	Granuloma	—	—	—

—: no remarkable change; ±: minimal change; +: mild change; and ++: moderate change.

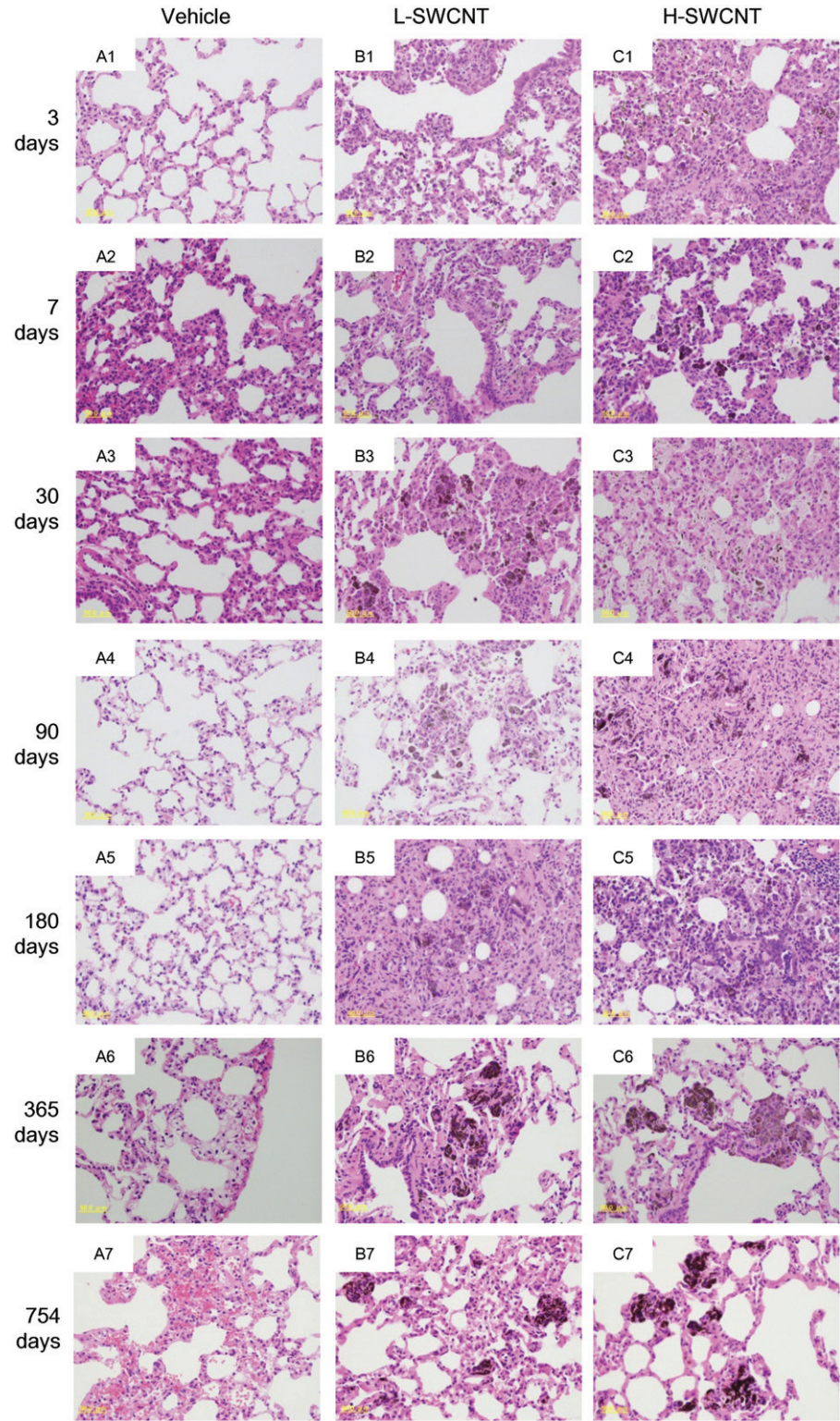
groups during the observation period, while no obvious morphological changes were observed in the vehicle control group. The appearance of the SWCNT aggregates resulted in a time-dependent decrease in each group (Figure 2). Histopathological findings of lungs stained with hematoxylin and eosin showed that fine granular substances, which were phagocytosed by persistent alveolar macrophages, were observed in the alveoli, alveolar wall and bronchioles in both SWCNT groups during the observation period (Table 1 and Figure 3). Persistence of macrophages laden with SWCNT aggregates as granular substances was observed in the alveolar walls and alveoli at three days post-instillation in both SWCNT groups (Figure 3B1 and C1), at seven days post-instillation in both SWCNTs groups (Figure 3B2 and C2) and at 30 days post-instillation in the L-SWCNT group (Figure 3B3). However, inflammatory cell infiltration was barely discerned in each of the experimental groups. A pale-pink fibrin deposition was observed in pulmonary alveoli at 30 days post-instillation in the H-SWCNT group (Figure 3C3). Persistence of macrophages laden with SWCNT aggregates as granular substances was observed in the alveolar walls and alveoli at 90 days

post-instillation in the L-SWCNT group (Figure 3B4). The proliferation of collagen fibers in the persistent alveolar macrophage-containing granuloma around the sites of SWCNT aggregates was observed at 90 days post-instillation in the H-SWCNT group (Figure 3C4). Macrophage-containing granuloma or foamy alveolar macrophage-containing granuloma around the sites of SWCNT aggregates was observed at 180 days post-instillation in the L-SWCNT or H-SWCNT group, respectively (Figure 3B5 and C5). Persistent macrophage-containing SWCNT aggregates as granular substances were diffusely localized in the alveolar walls and alveoli at 365 or 754 days post-instillation in both SWCNT groups (Figure 3B6, C6, B7 and C7). Masson's trichrome staining confirmed the absence of fibrotic lesions in each of the experimental groups (Supplementary Figure 1).

Gene expression analysis

Comprehensive analysis of gene expression profiles was performed using a DNA microarray. The numbers of significantly expressed genes at each time point, including overlapping

Figure 3. Micrographs of lung tissue from a rat exposed to SWCNTs at 3, 7, 30, 90, 180, 365 and 754 days post-instillation. After the rats were sacrificed, the lung tissues were fixed in 4% buffered paraformaldehyde, followed by embedding in paraffin, and the sections were stained with hematoxylin and eosin.



sequences between L-SWCNT and H-SWCNT groups, are shown in Figure 4. The number of upregulated genes markedly increased at seven days post-instillation, followed by a gradual decrease up to 180 days post-instillation. The number of upregulated genes increased at 365 days post-instillation. These results suggest that there existed a transition period between 180 and 365 days post-instillation in the gene expression profiles. Therefore, we displayed the time-dependent change in statistically overrepresented GO terms of genes upregulated by H-SWCNTs. As a consequence of this transition, inflammatory response-associated GO terms were significantly overrepresented (Table 2). The GO categories involved in the “inflammatory response” (GO:

0006954), “chemotaxis” (GO: 0006935), “leukocyte chemotaxis” (GO: 0030595), “leukocyte migration” (GO: 0050900), “defense response” (GO: 0006952), “immune system process” (GO: 0002376) and “cell proliferation” (GO: 0008283) displayed extremely low *p* values [synonym: high-log (*p* value)] until 180 days post-instillation in the H-SWCNT group (Figure 5). On the other hand, the *p* values were very high at the 365- or 754-day post-instillation periods. The GO categories with extremely low *p* values [e.g. inflammatory response (GO: 0006954) and chemotaxis (GO: 0006935)] were not overrepresented at 365 or 754 days post-instillation (data not shown). These results suggest that gene expression profiles associated with inflammatory response were

dramatically altered after 180 days post-instillation. Overall, a negative correlation between the numbers of upregulated and downregulated genes was observed at each time point. Downregulated genes were unable to be classified into defined GO categories based on the extremely low *p* value obtained in this study (data not shown).

A list of selected expressed genes involved in the inflammatory response after intratracheal instillation with SWCNTs is shown in Table 3. Genes encoding for the complement proteins C1qa, C3 and C4bpa involved in the innate immune response exhibited high-level induction until 90 or 180 days post-instillation in both SWCNT groups. In the L-SWCNT group, several genes were highly upregulated until 90 days post-instillation, including the chemokine (C–C motif) ligand gene, *Ccl2* (encoding for monocyte chemotactic protein 1, MCP1), *Ccl3* (encoding for macrophage inflammatory protein 1 alpha, MIP-1a), *Ccl7* (encoding for monocyte chemoattractant protein 3, MCP-3),

Ccl9, *Ccl12*, *Ccl17* (encoding for small inducible cytokine subfamily A member 17, SCYA17), *Ccl22* (encoding for SCYA22), the chemokine (C–X–C motif) ligand gene, *Cxcl2* (encoding for cytokine-induced neutrophil chemoattractant 3, CINC-3; macrophage inflammatory protein 2, Mip-2), *Cxcl3* (encoding for cytokine-induced neutrophil chemoattractant-2, CINC-2) and *Cxcl5* (encoding for granulocyte chemotactic protein 2, GCP-2). These genes were also upregulated by high-dose SWCNT up to 180 days. This result indicates that the regulation occurred in a dose-dependent manner. Alpha-1-acid glycoprotein 1 (encoded by *Orm1*), an acute-phase reactant protein, was markedly upregulated until 180 days post-instillation. Concomitantly, no representative genes involved in the inflammatory response were upregulated at 365 or 754 days post-instillation in either SWCNT group.

A list of selected expressed genes involved in the response to oxidative stress and apoptosis after intratracheal instillation with SWCNTs is shown in Table 4. The genes *Hmox1* and *Sod2* exhibited a similarly high expression pattern until 90 days post-instillation in both SWCNT groups, but the expression returned to nearly baseline levels at 180 days post-instillation. However, other representative genes involved in the response to oxidative stress – such as the genes *Cat*, *Gpx1*, *Gpx3*, *Gss* and *Sod1* – were scarcely altered in all time points. The expression of *Lcn2*, which encodes a member of the lipocalin superfamily with diverse functions – including regulation of inflammatory responses, control of cell growth and development, tissue involution and apoptosis – was markedly upregulated until 180 days post-instillation in both

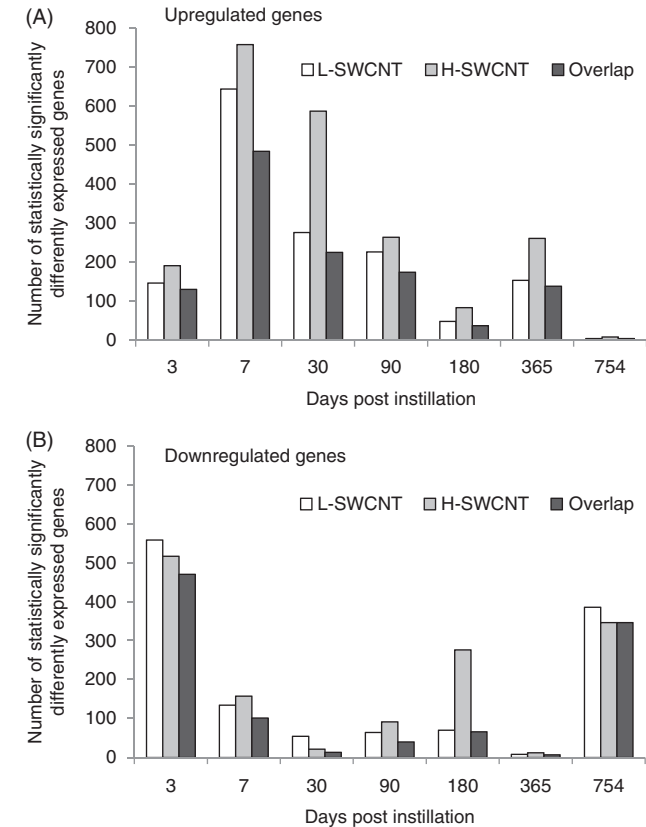


Figure 4. Genes with statistically significant upregulated/downregulated changes in expression at each time point in the L-SWCNT group and H-SWCNT group. Upregulated genes (A) or downregulated genes (B) with *p* values less than or equal to 0.05 at each time point, including overlaps between the L-SWCNT group and H-SWCNT group, were counted.

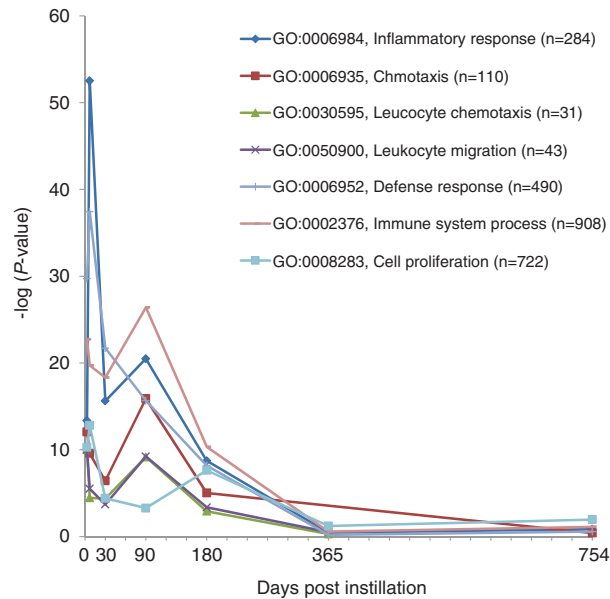


Figure 5. Time-dependent changes in *p* values of statistically over-represented GO terms of H-SWCNT-induced genes.

Table 2. Time-dependent changes in statistically overrepresented GO terms of H-SWCNT-induced genes.

GO ID	GO terms	Number in the group	Number changed						
			3 d	7 d	30 d	90 d	180 d	365 d	754 d
GO: 0006954	Inflammatory response	284	26	43	29	31	18	7	3
GO: 0006935	Chemotaxis	110	17	18	12	9	9	0	1
GO: 0030595	Leucocyte chemotaxis	31	10	7	6	9	4	1	0
GO: 0050900	Leukocyte migration	43	11	9	6	10	5	2	0
GO: 0006952	Defense response	490	34	51	31	33	22	10	3
GO: 0002376	Immune system process	908	44	59	42	42	27	21	7
GO: 0008283	Cell proliferation	722	29	44	23	18	21	21	8

Table 3. Selected list of expressed genes involved in inflammatory response after intratracheal instillation with SWCNTs.

GenBank	Gene name	L-SWCNT							H-SWCNT							Description
		3 d	7 d	30 d	90 d	180 d	365 d	754 d	3 d	7 d	30 d	90 d	180 d	365 d	754 d	
NM_001008515	C1qa	0.8	<i>1.2</i>	<i>1.1</i>	<i>0.7</i>	0.3	0.0	0.4	0.8	<i>1.6</i>	1.2	<i>1.1</i>	1.0	0.3	<i>0.4</i>	Complement component 1, q subcomponent, A chain
NM_016994	C3	<i>1.5</i>	<i>1.0</i>	<i>1.9</i>	<i>1.4</i>	0.5	0.1	−0.1	<i>1.6</i>	<i>1.4</i>	<i>1.5</i>	<i>1.9</i>	<i>1.3</i>	0.1	−0.2	Complement component 3
NM_012516	C4bpa	<i>1.3</i>	<i>1.6</i>	<i>1.8</i>	<i>1.3</i>	0.4	0.3	0.1	<i>1.4</i>	<i>2.2</i>	1.6	<i>1.5</i>	1.1	0.3	0.2	Complement component 4 binding protein, alpha
NM_016995	C4bpb	<i>0.6</i>	<i>1.0</i>	1.3	0.9	0.3	<i>0.5</i>	−0.1	<i>0.9</i>	1.2	1.2	<i>1.3</i>	0.5	<i>0.6</i>	−0.2	Complement component 4 binding protein, beta
NM_031530	Ccl2	2.0	<i>2.4</i>	<i>2.4</i>	<i>2.4</i>	0.1	−0.1	0.1	<i>2.5</i>	<i>3.2</i>	<i>2.4</i>	<i>2.7</i>	1.1	0.2	0.4	Chemokine (c-c motif) ligand 2
NM_013025	Ccl3	1.1	1.3	<i>1.5</i>	<i>1.2</i>	0.2	−0.3	−0.4	<i>1.3</i>	<i>1.7</i>	1.3	<i>1.3</i>	0.9	0.0	−0.2	Chemokine (c-c motif) ligand 3
NM_053858	Ccl4	<i>0.6</i>	<i>0.9</i>	<i>1.3</i>	0.6	0.0	−0.1	−0.2	<i>0.7</i>	<i>1.0</i>	0.7	0.6	0.4	−0.1	−0.1	Chemokine (c-c motif) ligand 4
NM_031116	Ccl5	0.2	−0.1	0.2	0.0	−0.3	−0.1	−0.1	0.0	0.0	−0.2	−0.3	0.1	0.0	−0.2	Chemokine (c-c motif) ligand 5
NM_001007612	Ccl7	1.9	<i>2.8</i>	<i>3.2</i>	<i>2.2</i>	0.1	−0.4	−0.1	<i>2.5</i>	<i>3.7</i>	3.3	<i>2.9</i>	1.5	0.0	0.4	Chemokine (c-c motif) ligand 7
NM_001012357	Ccl9	0.5	0.9	<i>1.6</i>	1.0	<i>0.6</i>	0.1	0.2	0.3	<i>1.0</i>	1.3	<i>1.2</i>	<i>1.1</i>	0.1	0.5	Chemokine (c-c motif) ligand 9
NM_001105822	Ccl12	1.6	1.8	<i>2.0</i>	<i>2.1</i>	−0.6	−0.6	0.3	<i>2.3</i>	<i>2.7</i>	1.8	<i>2.2</i>	0.3	−0.8	0.3	Chemokine (c-c motif) ligand 12
NM_057151	Ccl17	<i>2.1</i>	<i>1.7</i>	<i>1.3</i>	1.0	0.1	−0.8	0.0	<i>2.3</i>	<i>2.0</i>	0.8	<i>1.4</i>	0.7	−0.9	0.4	Chemokine (c-c motif) ligand 17
NM_057203	Ccl22	<i>4.0</i>	<i>2.7</i>	<i>2.3</i>	<i>1.7</i>	0.8	−0.2	−0.5	<i>4.0</i>	<i>3.4</i>	<i>2.0</i>	<i>2.4</i>	1.6	0.2	0.3	Chemokine (c-c motif) ligand 22
NM_030845	Cxcl1	1.7	0.6	0.3	0.7	0.2	−0.4	0.5	1.8	0.6	−0.2	0.7	0.6	−0.7	0.3	Chemokine (c-x-c motif) ligand 1
NM_053647	Cxcl2	1.8	0.8	0.3	1.4	0.3	−0.7	0.3	<i>2.2</i>	1.5	0.2	1.5	1.0	−0.8	0.6	Chemokine (c-x-c motif) ligand 2
NM_138522	Cxcl3	<i>1.6</i>	0.7	<i>1.1</i>	0.7	0.1	0.2	0.1	<i>1.8</i>	<i>1.1</i>	0.8	<i>1.2</i>	0.7	−0.2	−0.1	Chemokine (c-x-c motif) ligand 3
NM_022214	Cxcl5	1.3	0.6	<i>1.6</i>	1.9	−0.8	−0.6	−0.1	1.7	0.6	2.1	<i>2.2</i>	0.0	0.3	−0.2	Chemokine (c-x-c motif) ligand 5
NM_053958	Ccr3	1.0	0.3	0.2	−0.8	0.8	0.1	−0.8	1.3	0.7	−0.1	−0.7	0.6	0.2	0.1	Chemokine (c-c motif) receptor 3
NM_133532	Ccr4	<i>2.0</i>	<i>3.4</i>	1.8	0.8	0.0	−0.3	0.4	1.8	<i>3.6</i>	1.8	1.2	0.2	0.2	−0.3	Chemokine (c-c motif) receptor 4
NM_053288	Orm1	<i>3.6</i>	<i>3.4</i>	<i>3.3</i>	<i>3.7</i>	2.6	0.2	−0.7	<i>3.9</i>	<i>3.6</i>	2.9	<i>4.7</i>	<i>4.4</i>	0.7	0.8	Orosomucoid 1

Numerical values represent gene expression log-fold change compared to control levels. Log fold changes with *p* values less or equal than 0.05 are shown in italics.

Table 4. Selected list of expressed genes involved in response to oxidative stress and apoptosis after intratracheal instillation with SWCNTs.

Genbank	Gene name	L-SWCNT							H-SWCNT							Description
		3 d	7 d	30 d	90 d	180 d	365 d	754 d	3 d	7 d	30 d	90 d	180 d	365 d	754 d	
NM_030826	Gpx1	0.0	0.0	0.4	0.1	0.0	<i>0.1</i>	0.1	0.1	0.4	0.3	0.1	<i>0.3</i>	0.1	−0.1	Glutathione peroxidase 1
NM_022525	Gpx3	−0.2	−0.5	0.1	−0.5	−0.1	−0.2	0.1	−0.2	−0.6	−0.1	−0.3	0.2	−0.2	0.0	Glutathione peroxidase 3
NM_012962	Gss	<i>0.3</i>	−0.2	<i>0.5</i>	0.1	0.1	0.0	0.1	<i>0.3</i>	0.2	0.4	0.4	0.4	0.0	0.0	Glutathione synthetase
NM_012580	Hmox1	0.5	0.6	<i>1.5</i>	<i>1.0</i>	0.4	0.1	−0.7	0.6	<i>1.1</i>	1.5	<i>1.4</i>	0.9	0.3	0.4	Heme oxygenase (decycling) 1
NM_017050	Sod1	0.1	−0.2	0.2	−0.2	−0.1	−0.1	0.0	0.1	0.1	−0.1	−0.1	0.2	−0.2	0.0	Superoxide dismutase 1
NM_017051	Sod2	<i>1.1</i>	1.0	<i>1.3</i>	<i>1.0</i>	0.1	−0.1	0.1	<i>1.1</i>	<i>1.1</i>	1.3	1.0	0.4	0.1	0.2	Superoxide dismutase 2, mitochondrial
NM_012762	Casp1	−0.1	0.0	0.0	−0.2	−0.1	0.0	0.0	−0.1	0.0	−0.2	−0.4	0.0	<i>0.2</i>	0.0	Caspase 1
NM_022522	Casp2	0.1	0.0	0.0	−0.1	0.0	0.1	0.0	0.0	0.2	−0.2	−0.2	0.2	0.1	0.0	Caspase 2
NM_012922	Casp3	−0.1	−0.1	0.0	0.0	0.1	0.1	0.1	−0.1	−0.1	0.0	−0.1	0.0	0.2	0.0	Caspase 3
NM_053736	Casp4	<i>0.4</i>	0.3	0.2	0.1	−0.2	0.1	0.1	<i>0.3</i>	0.6	0.1	0.4	0.1	0.1	0.0	Caspase 4
NM_022260	Casp7	0.1	0.1	0.1	−0.1	−0.3	0.1	0.0	0.1	0.3	−0.1	−0.2	0.0	0.1	0.0	Caspase 7
NM_022277	Casp8	0.3	0.2	0.4	−0.1	0.1	0.1	0.0	0.2	0.3	0.1	−0.2	0.3	<i>0.2</i>	−0.1	Caspase 8
NM_130422	Casp12	0.1	−0.1	0.0	−0.2	0.0	0.0	0.1	0.1	0.1	−0.3	−0.2	0.1	−0.2	0.0	Caspase 12
NM_012520	Cat	0.2	−0.3	0.6	−0.2	0.2	0.2	0.2	0.1	0.2	0.3	0.0	<i>0.6</i>	<i>0.1</i>	0.1	Catalase
NM_130741	Lcn2	<i>2.8</i>	<i>2.7</i>	<i>3.6</i>	<i>2.9</i>	1.3	0.8	0.1	<i>3.0</i>	<i>3.2</i>	3.3	<i>3.5</i>	2.5	0.9	0.2	Lipocalin 2

Numerical values represent gene expression log fold change compared to control levels. Log fold changes with *p* values less or equal than 0.05 are shown in italics.

SWCNT groups. Overall, none of the representative genes associated with apoptosis displayed a high degree of induction in either of the SWCNT groups. Other representative genes involved in apoptosis, such as the *Casp1*, *Casp2*, *Casp3*, *Casp4*, *Casp7*, *Casp8* and *Casp12* genes encoding members of the cysteine–aspartic acid protease (caspase) family, were barely altered in all time points.

DNA microarray and qRT-PCR assays demonstrated that genes were markedly upregulated during the observation period in the H-SWCNT group (Table 5). The expression levels of the genes *Ctsk*, *Gcgr*, *Gpnmb*, *Lilrb4*, *Marco*, *Mreg*, *Mt3*, *Padi1*, *Slc26a4*, *Spp1*, *Tnfsf4* and *Trem2* were persistently upregulated in a dose-dependent manner until 365 days post-instillation. In addition, the expression levels of *Atp6v0d2*, *Lpo*, *Mmp7*, *Mmp12* and *Rnase9* were significantly upregulated until 754 days post-instillation. The representative persistently downregulated genes involved in the inflammatory response, oxidative stress and apoptosis are not presented (the Gene Expression Omnibus database, Accession number GSE50664).

MMP12, MMP7 and SPP1 immunostaining

Several genes were markedly upregulated during the observation period in the H-SWCNT group (Table 5), including the genes encoding macrophage metalloelastase (*Mmp12*), matrilysin (*Mmp7*), and secreted phosphoprotein 1 (*Spp1*). These persistently upregulated genes may act as potential biomarkers in the chronic-phase response following the acute-phase response in lung tissue after SWCNT instillation. To verify the validity of these results and to observe the localization of these gene products in lung tissue, we performed immunostaining with anti-MMP12, -MMP7 or -SPP1 antibodies, respectively. The induction of MMP12 was observed in bronchial epithelial cells until 30 days post-instillation and in alveolar macrophages during the observation period in both SWCNT groups. Furthermore, MMP12 was markedly induced in foamy alveolar macrophages at 90 days post-instillation (Figure 6). By contrast, no induction of MMP7 in bronchial epithelial cells or alveolar macrophages was observed during the observation period in either of the experimental groups (data not shown). One likely explanation is that MMP7 was induced, but not at detectable levels. Finally, SPP1 was induced in alveolar macrophages during the observation period in both SWCNT groups, and was markedly induced in foamy alveolar macrophages at 90 days post-instillation (Figure 7).

Discussion

Several studies have reported histopathological findings of granuloma formation in mouse or rat lungs after intratracheal instillation in SWCNTs. Lam et al. (2004) investigated the toxicity of SWCNTs using mice exposed to three different types of SWCNTs at two concentrations (0.1 mg or 0.5 mg) by intratracheal instillation. The mice were toxicologically assessed 7 or 90 days post-instillation. The SWCNTs studied generated persistent epithelioid granulomas (associated with particle agglomerates) in the 0.5 mg SWCNT groups and induced dose-dependent interstitial inflammation (Lam et al., 2004). Warheit et al. (2004) used intratracheal instillation to expose rats to SWCNTs (nominal diameters of 1.4 nm and lengths > 1 µm) at concentrations of 1.0 mg/kg or 5.0 mg/kg, and evaluated their effects at 24 h, one week, one month and three months post-exposure. A transient inflammatory response in the lung (observed up to one month post-exposure) and dose-independent, non-uniformly distributed multifocal granulomas were observed (Warheit et al., 2004). In addition, Kobayashi et al. (2011) used intratracheal instillation to expose rats to highly pure SWCNTs at concentrations of 0.04 mg/kg, 0.2 mg/kg or 1.0 mg/kg and

evaluated their effects at three days, one week, one month, three months and six months post-exposure. Consequently, inflammatory cell infiltration in the alveolus and granuloma were observed up to three months post-exposure (Kobayashi et al., 2011). Chou et al. (2008) reported that SWCNT-induced pathogenesis in the lungs of mice was observed in both early (i.e. less than three days) and late (i.e. 14 days) responses. During the early response phase, the histological data revealed an increase in macrophage infiltration and formation of SWCNT-loaded, foamy-like macrophages in the alveolar space, whereas no significant granuloma formation occurred. The pulmonary granulomas could be identified primarily after one week of SWCNT treatment, and profound multifocal granulomas were observed after 14 days (Chou et al., 2008). The granulomas may display unique histopathological signs of toxicity for SWCNTs, although the mechanisms involved in granuloma formation remain unclear. Lam et al. (2004) suggested that CNTs were capable of inducing granulomas in mice or rats; their findings, together with a report from Warheit et al. (2004), are suggestive of a fundamental difference between the unique physicochemical properties of CNTs and those of carbon black, i.e. granulomas were not observed in rodents exposed to carbon black. The investigators proposed that granulomas could impair cellular and physiological (gas exchange) lung functions, generating fibrosis, more defined nodules and additional lesions (Lam et al., 2004). In addition, granuloma formation around the activated macrophages may play a role in protecting the surrounding host tissue from destructive chronic inflammation. Alveolar macrophages appear to initiate SWCNT-induced pathogenesis through SWCNT phagocytosis, followed by the release of a variety of cytokines to recruit distinct immune cells and granuloma formation (Chou et al., 2008). In this study, the persistence of alveolar macrophage-containing granulomas was observed around the SWCNT aggregate sites following fibrin deposition at 90 days post-instillation in the H-SWCNT group. On the basis of the aforementioned studies, we suggest that the histopathological signs of our study resulted from a transition period from the acute-phase to the subchronic-phase response in SWCNTs, a transition period that was estimated to occur at 90 days post-instillation in the H-SWCNT group.

Next, we addressed the time-dependent changes in gene expression profiling in connection with the histopathological results, proposing a transition model for gene expression patterns in the pulmonary region after intratracheal instillation with SWCNTs. Gene expression data showed that upregulated genes were statistically overrepresented in GO categories involved in “inflammatory response”, “chemotaxis” and “defense response” until 90 days post-instillation. In addition, representative genes (e.g. *C1qa*, *C3*, *C4bpa*, *C4bpb*, *Ccl2*, *Ccl3*, *Ccl7*, *Ccl9*, *Ccl12*, *Ccl17*, *Ccl22*, *Cxcl2*, *Cxcl3*, *Cxcl5* and *Orml1*) involved in the inflammatory response were upregulated at 90 days post-instillation in the H-SWCNT group. The gene expression profiles suggest that pulmonary acute-phase response persists up to at least 90 days after intratracheal instillation in this experimental setting. We previously reported that some genes were identified as potential biomarkers in acute-phase responses after intratracheal instillation with C₆₀ fullerenes in lung tissues (Fujita et al., 2010). Interestingly, the *C3*, *C4bpa*, *Ccl2*, *Ccl3*, *Ccl7*, *Ccl9*, *Ccl22*, *Cxcl2*, *Cxcl3*, *Cxcl5*, *Ccr4* and *Orml1* genes were all upregulated in response to C₆₀ fullerene treatment in the acute phase (seven days post-instillation) in a dose-dependent manner, which overlapped with those of representative genes upregulated in the H-SWCNT group until 90 days post-instillation. It is likely that these genes were specifically expressed by carbon-based nanomaterials. To address this issue, gene expression profiling data for other nanomaterials should be evaluated in future studies and the selected genes should be individually examined.

Table 5. Selected list of markedly up-regulated genes during the observation period in the L-SWCNT and H-SWCNT group.

GenBank	Gene name	L-SWCNT (DNA microarray)					H-SWCNT (DNA microarray)					H-SWCNT (qRT-PCR)					Description
		3 d	7 d	30 d	90 d	180 d	365 d	754 d	3 d	7 d	30 d	90 d	180 d	365 d	754 d		
NM_001011972	Atp6v0d2	2.5	3.3	4.3	3.6	2.6	1.6	0.7	2.7	3.8	4.3	4.0	3.6	2.0	1.4	5.3	ATPase, h+ transporting, lysosomal v0 subunit d2
NM_031560	Ctsk	−0.4	1.4	1.3	1.6	0.8	0.6	0.1	−0.2	1.0	2.0	1.6	1.0	1.4	0.5	1.1	Cathepsin k
NM_172091	Gcgr	0.2	0.6	1.8	1.8	1.5	1.7	1.1	0.5	1.2	1.9	2.6	2.7	1.8	1.8	0.9	Glucagon receptor
NM_133298	Gpnmb	0.7	1.4	2.2	1.7	1.3	0.8	0.5	0.8	1.9	2.4	2.1	2.2	1.0	0.9	2.2	Glycoprotein (transmembrane) nmb
NM_001013894	Lilrb4	1.1	1.1	1.9	1.1	0.5	0.9	0.0	0.9	1.6	2.1	1.5	1.6	1.3	0.7	1.9	Leukocyte immunoglobulin-like receptor, subfamily b, member 4
NM_001105829	Lpo	2.8	3.9	6.0	6.0	3.8	0.8	0.0	3.0	4.6	6.0	6.9	5.7	2.5	1.2	2.8	Lactoperoxidase
NM_001109011	Marco	0.8	2.6	2.6	3.8	0.2	0.4	−0.6	1.2	2.6	2.5	4.9	1.0	1.7	−0.2	2.4	Macrophage receptor with collagenous structure
NM_012864	Mmp7	2.4	4.3	4.4	4.1	2.4	3.5	2.4	3.1	5.2	4.9	4.6	3.5	4.2	2.8	7.1	Matrix metalloproteinase 7
NM_053963	Mmp12	1.6	3.6	3.9	3.4	2.1	1.6	0.7	1.8	4.0	3.9	4.1	3.4	2.2	1.4	3.4	Matrix metalloproteinase 12
NM_001192002	Mreg	1.9	2.3	1.9	2.8	0.7	1.1	0.1	2.1	2.8	1.8	3.0	1.9	1.4	0.2	2.0	Melanoregulin
NM_053968	Mt3	0.1	0.6	0.9	1.5	3.0	3.1	1.8	0.4	0.8	1.1	2.1	4.0	3.1	2.5	5.4	Metallothionein 3
NM_019332	Padl1	2.1	2.8	1.4	1.2	0.4	0.6	0.2	2.8	3.5	1.8	2.2	1.4	1.5	0.2	2.6	Peptidyl arginine deiminase, type i
NM_001008561	Rnase9	1.9	4.3	2.9	1.9	2.0	1.6	1.4	1.2	3.6	2.0	2.4	3.3	1.2	1.7	1.2	Ribonuclease, RNase a family, 9
NM_019214	Slc26a4	2.4	3.0	3.4	3.2	0.9	0.7	−0.3	2.8	3.6	3.4	3.5	2.0	1.2	0.0	1.8	Solute carrier family 26, member 4
NM_012881	Spp1	1.8	2.5	3.3	3.2	2.1	0.9	0.4	2.3	3.3	3.8	3.6	3.3	1.6	0.9	1.4	Secreted phosphoprotein 1
NM_053552	Tnfrsf4	2.5	3.3	0.7	1.6	0.1	1.1	0.4	2.3	4.0	0.7	1.1	0.4	1.4	0.8	0.6	Tumor necrosis factor (ligand) superfamily, member 4
NM_001106884	Trem2	1.3	2.1	3.5	2.1	1.2	1.2	−0.1	1.3	2.4	3.0	2.6	2.3	1.7	0.3	1.9	Triggering receptor expressed on myeloid cells 2

Numerical values represent gene expression log-fold change compared to control levels. Log-fold changes with *p* values less or equal than 0.05 are shown in italics.

Figure 6. MMP12 immunostaining in lung tissues intratracheally instilled with vehicle control (A1 and A2), L-SWCNT (B1 and B2) or H-SWCNT (C1 and C2) at 90 days post-instillation.

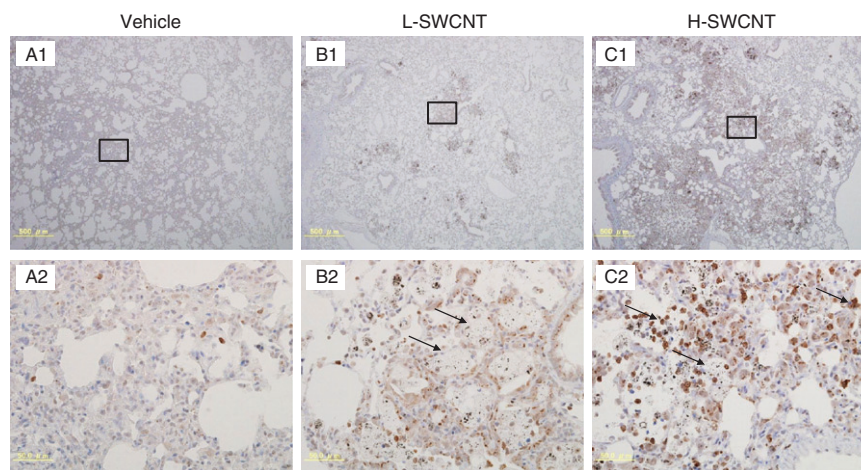
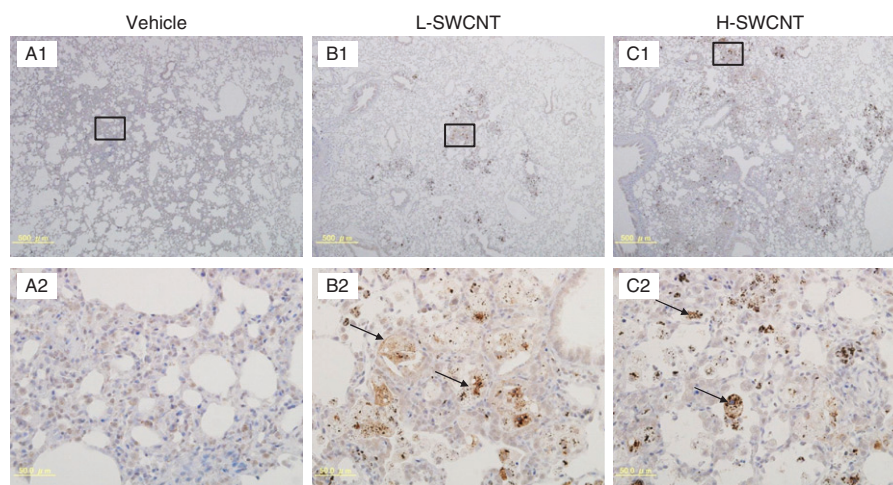


Figure 7. SPP1 immunostaining in lung tissues intratracheally instilled with vehicle control (A1 and A2), L-SWCNT (B1 and B2) or H-SWCNT (C1 and C2) at 90 days post-instillation.



The *Hmox1* and *Sod2* genes were upregulated until 90 days post-instillation, but their expression levels returned to nearly baseline at 180 days post-instillation. The *Hmox1* and *Sod2* genes may be upregulated by SWCNTs as an anti-oxidative defense factor occurring during lung injury in the acute-phase period. *Hmox1* gene expression in rat lungs was increased during the acute and chronic phases of crystalline silica or chrysotile asbestos exposure (Nagatomo et al., 2006, 2007). We previously observed changes in the expression of *Hmox1* and *Sod2* genes in response to exposure to ultrafine nickel oxides (Fujita et al., 2009b). However, the expression of genes involved in the oxidative stress response by SWCNTs has not been reported in *in vivo* animal tests. In order to better understand the role of the expression of genes involved in the oxidative stress response – specifically, SWCNT-induced apoptosis – further information regarding the *in vivo* mechanisms of SWCNT action is required.

The *Atp6v0d2*, *Lpo*, *Mmp7*, *Mmp12* and *Rnase9* genes were markedly upregulated during the observation period. It has been reported that *Atp6v0d2* is an essential component of the osteoclast-specific proton pump that mediates extracellular acidification during bone resorption (Wu et al., 2009). At the transcriptional level, *Rnase9* was expressed in a wide variety of tissues (Liu et al., 2008). However, the mechanism responsible for pulmonary inflammation was unknown. *Rnase9* expression was upregulated by C_{60} fullerenes, with expression levels that were positively correlated with the dosage of C_{60} fullerenes at six months post-instillation (Fujita et al., 2010).

We previously reported that the *Mmp12* and *Mmp7* genes were persistently expressed at high levels for six months

post-instillation in the presence of 1.0 mg C_{60} fullerenes (Fujita et al., 2010). It is noteworthy that the upregulation continued for six months post-instillation. These results suggested the existence of a long-term effect of C_{60} fullerene particles on the pulmonary interstitium, both on the alveolar septa in a restricted sense and on the interstitial spaces of the lungs in a more general sense. Similarly, *Mmp12* and *Mmp7* were markedly upregulated by SWCNTs during the observation period in this study. Furthermore, induction of MMP12 was observed in bronchial epithelial cells until 30 days post-instillation and in alveolar macrophages during the observation period in both of the SWCNT groups. MMP12 was markedly induced in foamy alveolar macrophages at 90 days post-instillation. Histopathological findings showed the presence of persistent macrophages laden with SWCNT aggregates as granular substances in the alveolar walls and alveoli during the entire observation period in both SWCNT groups. Proteolytic degradation and remodeling of the extracellular matrix (ECM) components by MMPs is essential for recovering from cellular damage (Shapiro, 1998). We surmise that the alveolar macrophages, which are activated by phagocytosis of SWCNT aggregates, constitutively induce MMP12 and MMP7 secretion to degrade ECM components in the alveoli for remodeling during the observation period.

SPP1 [also known as osteopontin (OPN)], a secreted chemokine-like protein that is a member of the small integrin-binding ligand N-linked glycoprotein (SIBLING) family, is synthesized by multiple cell types, including osteoclasts, activated T cells and activated macrophages. *Spp1* genes were markedly

upregulated by SWCNTs until 365 days post-instillation in the H-SWCNT group. Furthermore, SPP1 induction was observed in bronchial epithelial cells during the observation period, although little is known about the biological role of SPP1 in severe lung injury. However, Takahashi et al. (2001) demonstrated a dramatic increase in SPP1-expressing cells after instillation of bleomycin-induced fibrosis in mice. SPP1 may function as a multifunctional protein with cytokine/chemokine-like properties, as well as a fibrogenic cytokine that promotes migration, adhesion and proliferation of fibroblasts in pulmonary fibrosis in response to SWCNTs.

Conclusions

Several investigators have demonstrated that CNTs are capable of eliciting toxicity, including the initiation of an acute, neutrophil-driven inflammatory response, oxidative stress, granuloma formation and fibrosis. Therefore, broad conclusions may be postulated regarding the mechanisms underlying CNT toxicity (Johnston et al., 2010). We, in this study, illustrated an approach in investigating CNT toxicity using time-dependent changes in gene expression, together with histopathological and immunohistochemistry findings, to propose possible underlying mechanisms in pulmonary post-intratracheal instillation with SWCNTs. This study suggests that gene expression profiling provides valuable insight for integration of each toxicological endpoint. Furthermore, gene expression profiling data may be applicable for multiple distinct organs of the same species, providing a useful bridge between *in vitro* and *in vivo* testing. Moreover, gene expression profiling using GO analysis could prove to be beneficial for comparative analyses between different species.

Declaration of interest

There are no conflicts of interest to declare.

This research was funded by New Energy and Industrial Technology Development Organization of Japan (NEDO) grants “Evaluating risks associated with manufactured nanomaterials (P06041)” and “Innovative carbon nanotubes composite materials project toward achieving a low-carbon society (P10024)”.

References

- Beissbarth T, Speed TP. 2004. GStat: find statistically over-represented Gene Ontologies within a group of genes. *Bioinformatics* 12:1464–5.
- Cavallo D, Fanizza C, Ursini CL, Casciardi S, Paba E, Ciervo A, et al. 2012. Multi-walled carbon nanotubes induce cytotoxicity and genotoxicity in human lung epithelial cells. *J Appl Toxicol* 32:454–64.
- Chou CC, Hsiao HY, Hong QS, Chen CH, Peng YW, Chen HW, Yang PC. 2008. Single-walled carbon nanotubes can induce pulmonary injury in mouse model. *Nano Lett* 8:437–45.
- Davoren M, Herzog E, Casey A, Cottineau B, Chambers G, Byrne HJ, Lyng FM. 2007. In vitro toxicity evaluation of single walled carbon nanotubes on human A549 lung cells. *Toxicol In Vitro* 21: 438–48.
- Fujita K, Fukuda M, Endoh S, Kato H, Maru J, Nakamura A, et al. 2013. Physical properties of single-wall carbon nanotubes in cell culture and their dispersal due to alveolar epithelial cell response. *Toxicol Mech Methods* 23:598–609.
- Fujita K, Morimoto Y, Endoh S, Uchida K, Fukui H, Ogami A, et al. 2010. Identification of potential biomarkers from gene expression profiles in rat lungs intratracheally instilled with C(60) fullerenes. *Toxicology* 274:34–41.
- Fujita K, Morimoto Y, Ogami A, Myojyo T, Tanaka I, Shimada M, et al. 2009a. Gene expression profiles in rat lung after inhalation exposure to C60 fullerene particles. *Toxicology* 258:47–55.
- Fujita K, Morimoto Y, Ogami A, Tanaka I, Endoh S, Uchida K, et al. 2009b. A gene expression profiling approach to study the influence of ultrafine particles on rat lungs. In Kim JY, Platt U, Gu MB, & Iwahashi H, eds. *Atmospheric and Biological Environmental Monitoring*. The Netherlands: Springer-Verlag GmbH, 221–9.
- Guo NL, Wan YW, Denvir J, Porter DW, Pacurari M, Wolfarth MG, et al. 2012. Multiwalled carbon nanotube-induced gene signatures in the mouse lung: potential predictive value for human lung cancer risk and prognosis. *J Toxicol Environ Health A* 75:1129–53.
- Haniu H, Saito N, Matsuda Y, Tsukahara T, Maruyama K, Usui Y, et al. 2013. Culture medium type affects endocytosis of multi-walled carbon nanotubes in BEAS-2B cells and subsequent biological response. *Toxicol In Vitro* 27:1679–85.
- Hirano S, Fujitani Y, Furuyama A, Kanno S. 2010. Uptake and cytotoxic effects of multi-walled carbon nanotubes in human bronchial epithelial cells. *Toxicol Appl Pharmacol* 249:8–15.
- Johnston HJ, Hutchison GR, Christensen FM, Peters S, Hankin S, Aschberger K, Stone V. 2010. A critical review of the biological mechanisms underlying the in vivo and in vitro toxicity of carbon nanotubes: the contribution of physico-chemical characteristics. *Nanotoxicology* 4:207–46.
- Kobayashi N, Naya M, Mizuno K, Yamamoto K, Ema M, Nakanishi J. 2011. Pulmonary and systemic responses of highly pure and well-dispersed single-wall carbon nanotubes after intratracheal instillation in rats. *Inhal Toxicol* 23:814–28.
- Lam CW, James JT, McCluskey R, Hunter RL. 2004. Pulmonary toxicity of single-wall carbon nanotubes in mice 7 and 90 days after intratracheal instillation. *Toxicol Sci* 77:126–34.
- Liu J, Li J, Wang H, Zhang C, Li N, Lin Y, et al. 2008. Cloning, expression and location of RNase9 in human epididymis. *BMC Res Notes* 1:111.
- Ma-Hock L, Strauss V, Treumann S, Küttler K, Wohlleben W, Hofmann T, et al. 2013. Comparative inhalation toxicity of multi-wall carbon nanotubes, graphene, graphite nanoplatelets and low surface carbon black. *Part Fibre Toxicol* 10:23. doi: 10.1186/1743-8977-10-23.
- Ma-Hock L, Treumann S, Strauss V, Brill S, Luiz F, Mertler M, et al. 2009. Inhalation toxicity of multiwall carbon nanotubes in rats exposed for 3 months. *Toxicol Sci* 112:468–81.
- Mitchell LA, Gao J, Wal RV, Gigliotti A, Burchiel SW, McDonald JD. 2007. Pulmonary and systemic immune response to inhaled multi-walled carbon nanotubes. *Toxicol Sci* 100:203–14.
- Morimoto Y, Hirohashi M, Ogami A, Oyabu T, Myojo T, Todoroki M, et al. 2012a. Pulmonary toxicity of well-dispersed multi-wall carbon nanotubes following inhalation and intratracheal instillation. *Nanotoxicology* 6:587–99.
- Morimoto Y, Hirohashi M, Horie M, Ogami A, Oyabu T, Myojo T, et al. 2012b. Pulmonary toxicity of well-dispersed single-wall carbon nanotubes following intratracheal instillation. *J Nano Res* 18–19:9–25.
- Nagatomo H, Morimoto Y, Ogami A, Hirohashi M, Oyabu T, Kuroda K, et al. 2007. Change of heme oxygenase-1 expression in lung injury induced by chrysotile asbestos in vivo and in vitro. *Inhal Toxicol* 19: 317–23.
- Nagatomo H, Morimoto Y, Oyabu T, Hirohashi M, Ogami A, Yamato H, et al. 2006. Expression of heme oxygenase-1 in the lungs of rats exposed to crystalline silica. *J Occup Health* 48:124–8.
- Pauluhn J. 2010. Subchronic 13-week inhalation exposure of rats to multiwalled carbon nanotubes: toxic effects are determined by density of agglomerate structures, not fibrillar structures. *Toxicol Sci* 113: 226–42.
- Poland CA, Duffin R, Kinloch I, Maynard A, Wallace WA, Seaton A, et al. 2008. Carbon nanotubes introduced into the abdominal cavity of mice show asbestos-like pathogenicity in a pilot study. *Nat Nanotechnol* 3:423–8.
- Porter DW, Hubbs AF, Chen BT, McKinney W, Mercer RR, Wolfarth MG, et al. 2013. Acute pulmonary dose-responses to inhaled multi-walled carbon nanotubes. *Nanotoxicology* 7:1179–94.
- Sargent LM, Hubbs AF, Young SH, Kashon ML, Dinu CZ, Salisbury JL, et al. 2012. Single-walled carbon nanotube-induced mitotic disruption. *Mutat Res* 745:28–37.
- Shapiro SD. 1998. Matrix metalloproteinase degradation of extracellular matrix: biological consequences. *Curr Opin Cell Biol* 10:602–8.
- Stern ST, McNeil SE. 2008. Nanotechnology safety concerns revisited. *Toxicol Sci* 101:4–21.
- Takahashi F, Takahashi K, Okazaki T, Maeda K, Ienaga H, Maeda M, et al. 2001. Role of osteopontin in the pathogenesis of bleomycin-induced pulmonary fibrosis. *Am J Respir Cell Mol Biol* 24:264–71.
- Treumann S, Ma-Hock L, Gröters S, Landsiedel R, van Ravenzwaay B. 2013. Additional histopathologic examination of the lungs from

- a 90 days inhalation toxicity study with multiwall carbon nanotubes in rats. *Toxicol Sci* 134:103–10.
- Urankar RN, Lust RM, Mann E, Katwa P, Wang X, Podila R, et al. 2012. Expansion of cardiac ischemia/reperfusion injury after instillation of three forms of multi-walled carbon nanotubes. *Part Fibre Toxicol* 9:38. doi: 10.1186/1743-8977-9-38.
- Warheit DB, Laurence BR, Reed KL, Roach DH, Reynolds GA, Webb TR. 2004. Comparative pulmonary toxicity assessment of single-wall carbon nanotubes in rats. *Toxicol Sci* 77:117–25.
- Wu H, Xu G, Li YP. 2009. Atp6v0d2 is an essential component of the osteoclast-specific proton pump that mediates extracellular acidification in bone resorption. *J Bone Miner Res* 24:871–85.

Supplementary material available online

Supplementary Figure 1